PERFORMANCE EVALUATION OF FLAT WALLED DIFFUSER/NOZZLE MICROPUMP FOR FUEL DELIVERY IN SMALL GASOLINE ENGINE

First S.CHANDIKA Second R.ASOKAN
First: Asst. Professor (SG), Department of Mechatronics Engineering
Second: Professor & Head, Department of Information and Technology
Kongu Engineering College, Perundurai - 638 052, Erode, Tamilnadu, India.
Corresponding Author: chandika_2k3@yahoo.com, phone: +91 99650 56276

Abstract: *An investigation on flat-walled diffuser/nozzle micropump actuated by piezo-ceramic disc is presented towards the fuel delivery in a commercial 4 stroke, 125cc motorcycle. The flow directing ability of the valveless micropump primarily depends on the efficiency of the nozzle/diffuser elements. The diffuser efficiency is calculated from the total pressure loss coefficients. Numerical simulations are attempted to predict the flow characteristics of the diffuser/nozzle micropump using the microproduct design software INTELLISUITE. A breadboard circuit amplifier is developed to supply the high voltage electrical signal to the piezo-ceramic actuator. The numerically calculated flow characteristic of the proposed model is compared with the simulation results and experimental results.*

Key words: *diffuser/nozzle, piezo-ceramic disc, pressure loss coefficient, INTELLISUITE, amplifier*

1. Introduction

With advancement in microfabrication technologies, micropumps have received wide attention over the past three decades because of their possible applications in drug delivery, biological detection, cardiology system, chemical analysis, cooling of microelectronics, fuel injection etc. The micropump actuation mechanisms, fabrication technologies and applications are surveyed through several recent review articles [1-4].

Among several types of micropump, the most extensively investigated one is the reciprocating type. It consists of a flexible membrane and two passive check valves. The displacement of the membrane excited by the microactuators propels the flow. The main drawbacks of the passive check valves are valve clogging, wear, fatigue etc. In order to avoid the afore mentioned drawbacks, a novel design with valveless diffuser pump was first proposed by Van De Pol. Here, the passive check valves are replaced by nozzle/diffuser elements.

Subsequently, Stemme and Stemme developed diffuser/nozzle micropump and their result proved that the nozzle/diffuser pump provides a very good performance in terms of flow and pressure. Jiang et al. analyzed the performance of the diffuser/nozzle experimentally and attained the conclusion that the valveless design was feasible. Gerlach performed a pressure loss analysis on sharp and well rounded inlets for different diffuser angles.

In summary, the diffuser/nozzle pump has the following advantages: ease of manufacture as the design is simple and reliable, higher flow rate, possibility of usage at higher frequencies and hence, faster response time. In the last two decades, extensive research work has been carried out on the working characteristics and properties of the diffuser/nozzle micropumps. However, the flat walled nozzle/ diffuser has not received moderately as much attention. Hence, the performance evaluation of flat walled diffuser/ nozzle micropump towards the fuel delivery in a commercial 4 stroke, 125cc motorcycle is proposed.

As the Micro Electro Mechanical Systems (MEMS) technology continue to improve in recent years, many products can be mass-produced which in-turn reduces cost effectiveness with good product quality. With the MEMS as the driving constituent of recent techno-economy, this paper aims at the feasibility study on piezo-driven micropump for fuel delivery in automobiles. Metamorphosis operation of this micropump atomizes the fuel effectively for efficient mixing of fuel with atmospheric air for complete burning and the maximum utilization of fuel. Effective usage of fuel enhances the existence of fuel for many more years. This pervasive use of this technology not only uses the fuel completely through effective combustion, and hence, it indirectly reduces the emission of carbon monoxide (CO), carbon dioxide (CO_2) and prevents the destruction of ozone layer.

2. Fuel injection system

A detailed schematic of the fuel injection system proposed is shown in Fig. 1. A micropump can transfer mechanical energy into the fluid movement when the piezo-ceramic actuator is actuated by the control signal from the Electronic Control Unit (ECU), which consists of a small-programmed computer that translates sensor's signals into a command signals. The strength of the ECU control signal, which determines the required piezo-ceramic actuation voltage to control the amount of fuel injected, depends upon the engine requirements, which are determined by the ECU from the sensor's signals from critical locations. The sensory inputs given to the ECU are: engine speed sensor, oil temperature sensor, air temperature sensor, mass airflow rate sensor etc.

The configuration of the micropump proposed is shown in Fig. 2. The model of piezo actuated diffuser valve micropump consists of diffuser/nozzle element, inlet/outlet holes and the membrane which is actuated by a single layer disc type piezo ceramic disc bonded to the diaphragm. The pump utilizes the reciprocating motion of a membrane actuated by a piezo disc, to induce pumping action. To direct the flow, the diffuser and nozzle elements are used. This 3D model is developed using Solid works software [9].

3. Theoretical Analysis

3.1 Diffuser/Nozzle element

A diffuser is a device which transforms kinetic energy in the form of velocity into potential energy in the form of pressure [10]. Based on the divergence angle (2θ), the diffusers can be designed as wide angle diffuser (60 to 80 deg) and a narrow angle diffuser (4 to 10 deg). The rectification efficiency of wide-angle diffuser micropump is low due to the boundary layer separation along the diverging direction [1]. For this reason, currently most diffuser micropumps use narrow-angle diffusers, which are shown to have a better pump efficiency [11, 12]. The effects of the angles, lengths and throat/neck width of diffuser/nozzle elements on the velocity loss and flow rate are analyzed and optimized [13]. Hence, proposed diffuser/nozzle geometry are designed for L/W1=15, AR=3.8 and narrow-angle 2θ = 10°.

3.2 Pressure loss coefficient calculation

According to the work by Singhal et al., (2004) , Jiang et al., (1998) and Yang et al., (2008) the performance of a micropump depends on the characteristics of the diffuser/nozzle elements. The flow rate through diffuser/ nozzle elements can be evaluated from the pressure loss coefficients. The pressure loss coefficient (K) is used to calculate the diffuser efficiency which is given by [10]

$$K=\frac{\Delta p}{\rho v^2/2} \quad (1)$$

where Δp is the pressure drop across the diffuser or the nozzle direction, ρ is the fluid density and ν is the mean flow velocity. According to the literature work [12], the total pressure drop across the diffuser/nozzle element is divided into three parts as shown in Fig. 3: pressure drops due to sudden contraction at the throat (region 1), the sudden expansion at the exit (region 3) and the gradual expansion or contraction along the length of diffuser/nozzle elements (region 2) assuming negligible interference between these parts. Hence, the pressure drop across the diffuser direction ($\Delta p_{diff,t}$) and nozzle direction ($\Delta p_{nozz,t}$) are expressed as,

$$\Delta p_{diff,t} = \Delta p_{diff,th} + \Delta p_{diff,l} + \Delta p_{diff,ex} \quad (2)$$

$$\Delta p_{nozz,t} = \Delta p_{nozz,th} + \Delta p_{nozz,l} + \Delta p_{nozz,ex} \quad (3)$$

The pressure loss coefficient for the diffuser can be calculated as

$$K_{diff,t}=\frac{\Delta p_{diff,t}}{\frac{1}{2}\rho v_{th}^2} \quad (4)$$

$$=\frac{\Delta p_{diff,th}}{\frac{1}{2}\rho v_{th}^2}+\frac{\Delta p_{diff,l}}{\frac{1}{2}\rho v_{th}^2}+\frac{\Delta p_{diff,ex}}{\frac{1}{2}\rho v_{th}^2}\left(\frac{\rho v_{ex}^2/2}{\rho v_{th}^2/2}\right) \quad (5)$$

$$K_{diff,t}=K_{diff,th}+K_{diff,l}+K_{diff,ex}\frac{A_{th}^2}{A_{ex}^2} \quad (6)$$

Similarly, the total pressure loss coefficient for the nozzle (with respect to pressure head at the exit) is

$$K_{nozz,t}=\left(K_{nozz,th}+K_{nozz,l}\right)\frac{A_{th}^2}{A_{ex}^2}+K_{nozz,ex} \quad (7)$$

The pressure loss coefficient for gradually expanding diffuser or a gradually contracting nozzle is calculated as follows. The incompressible steady-flow energy equation in the diffuser direction (from cross section th to ex in Fig. 2.) reduces to

$$p_{th}+\frac{1}{2}\rho v_{th}^2=p_{ex}+\frac{1}{2}\rho v_{ex}^2+\Delta p_{diff,l} \quad (8)$$

$$\frac{\Delta p_{diff,l}}{\frac{1}{2}\rho v_{th}^2}=\frac{\left(p_{th}-p_{ex}\right)}{\frac{1}{2}\rho v_{th}^2}+\left(1-\frac{v_{ex}^2}{v_{th}^2}\right) \quad (9)$$

$$K_{diff,l}=1-\frac{A_{th}^2}{A_{ex}^2}-C_p \quad (10)$$

The losses are minimized when C_p is maximized. Hence, for the proposed diffuser geometry, the pressure loss coefficient is calculated from the pressure drop and the mean velocity at the exit. Similarly, the pressure loss coefficient in the nozzle direction (from cross section ex to th in Fig. 3.) is given by

$$K_{nozz,l}=\frac{\Delta p_{nozz,l}}{\rho v_{th}^2/2} \quad (11)$$

The diffuser/nozzle loss coefficient at various regions can be found in the literature is summarized in Table1.

3.3 Diffuser efficiency calculation

The diffuser efficiency (η) of the diffuser/nozzle element is defined as the ratio of pressure loss coefficients for the nozzle direction to that in the diffuser direction.

$$\eta=\frac{K_{nozz,t}}{K_{diff,t}} \quad (12)$$

To achieve the best flow directing capability, the diffuser efficiency should be as high as possible. The diffuser efficiency η of the proposed flat walled diffuser/nozzle element is calculated and it is summarized in Table 2.

Higher the C_p, better is the performance of the micropump. From the flat walled diffuser performance map, the maximum Cp occurs at 0.77. The pressure loss coefficients are calculated as in an internal flow system with turbulent flow considering flow channels and sudden expansion and contractions [10].

To achieve the best pump performance, the pressure losses in the diffuser direction should be minimized at the same time the losses in the nozzle direction are maximized [1]. The diffuser efficiency can also be increased by rounding the corners and smoothing the surface of the nozzle/diffuser structures [10]. The ratio between the pressure loss coefficients ($K_{nozz,t}/K_{diff,t}$) should be as high as possible in order to maximize the pumping stroke efficiency. The calculated diffuser efficiency for the proposed flat walled diffuser/nozzle micropump (area ratio AR=3.8) is 3.7. For an ideal case, the diffuser element efficiency of η=4.25 can be obtained when the area ratio is 1:5.

3.4 Flow rate calculation

In order to find the flow rate generated in the micropump, the stroke volume is calculated first. By integrating the central displacement equation, the stroke volume ΔV of the pumping chamber is obtained [9].

The theoretical maximum flow rate (Q) of the micropump depends on the stroke volume, efficiency of the diffuser/nozzle element and the applied frequency which can be calculated by the following equation [11]

$$Q = 2*\Delta V*f*C*60 \quad (13)$$

where, f is the frequency at which the pump works and C is the rectifying factor related to the structure of the nozzle/diffuser. The performance of a diffuser micropump is normally characterized by flow rectifying factor C, which is given by [8]

$$C=\frac{\eta^{0.5}-1}{\eta^{0.5}+1} \quad (14)$$

The rectification efficiency of nozzle-diffuser micropumps reported in the literature is very low, generally between 0.01 and 0.2.

Table 3 shows the theoretically calculated flow rates at a frequency range from 50 Hz to 540 Hz subjected to the applied voltage of 50 and 100 V. The maximum flow rate calculated is 9.89 ml/min when the applied voltage and frequency are 100 V and 540 Hz respectively.

4. Numerical simulations

The modeling and simulation of the piezo actuated diffuser/nozzle micropump (Fig. 5.) is done with the use of a microproduct design software package INTELLISUITE. The computer simulation tool INTELLISUITE is a software specifically created for MEMS design, simulation and optimization. It permits the modeling of various characteristics including mechanical, electrostatic and electromagnetic performance either in static or in dynamic mode. The micropump mask layout (shown in Fig. 4.) is created using an Intellimask module and the fabrication sequence is formed in Intellifab module. The micropump consists of a thin cylindrical chamber with membrane and two flat walled diffusers. Typical data of the micropump proposed is listed in Table 4.

The simulation is done through TEM (Thermoelectromechnical) analysis module. The piezo ceramic material is defined and their damping values are set as d3_11, d3_22 and d3_33 are -1e-4, -1e-4 and 3e-4 respectively. All the lateral faces of the membrane are anchored where the displacements and velocities are zero. The two fluid ports are defined as YZ fixed means that the fluid velocity in the Y and Z directions is held zero. The simulation is solved for the velocity in the X direction on the selected faces. The diaphragm moves upwards and downwards under the piezoelectric actuation. In the first half period, the diaphragm moves downwards which in turn increases the pressure of the pump chamber. Hence, the fluids are driven out from the chamber. In the second half period, the diaphragm moves upwards. Therefore, the pressure of pump chamber decreases which sucks the fluid in. The fluid properties such as viscosity and density of the fluid used are given in the fluid properties dialog box. The fluid used here is gasoline. The simulation results show (Fig. 6.) the relationship between the diaphragm amplitudes of the piezo actuator and the flow rate. The flow rates are obtained at a frequency of 540 Hz. As analyzed above, higher the input voltage to piezoelectric disc greater is the displacement and more fluid flows through the micropump.

5. Measurements Results and discussion

The validity of the proposed model is evaluated by comparing the simulation results in INTELLISUITE with the theoretical calculation and experimental results. Fig. 7. schematically depicts the experimental setup to elucidate the flow performance of the micropump in vitro. Gasoline is supplied from an inlet reservoir (glass cup) to the micropump. Tygon tubing with 2.4 mm in diameter and 980 mm in length is connected to both the inlet and the outlet. A sinusoidal voltage signal is generated from a function generator (APLAB Model FG3MD) and amplified by passing through a breadboard amplifier circuit. Then, the amplified voltage is applied to the piezo ceramic actuator. Hence, the flow rate is calculated by measuring the moving distance of the liquid surface for a given time. The experiment is carried out under various driven frequencies from 50 Hz to 650 Hz and applied sinusoidal voltages from 50 V to 100 V. To form a liquid-air interface in the Tygon tube, the gasoline fluid is infused into the micropump before the measurement is commenced. The volume flow rate Q is measured as [16]

$$Q=\pi d^2 \Delta x / 4\Delta t \quad (15)$$

where d is the diameter of the tube, Δx is the displacement during the time interval Δt. The maximum flow rate measured is 7.2 ml/min when the driving frequency and the voltage are 540 Hz and 100 V respectively. This satisfies the flow rate requirement in fuel delivery system of a commercial 4 stroke, 125cc motorcycle.

5.1 High voltage power supply

Piezo driven micropump requires a high voltage for operation. For signal conditioning and control requirements power amplifiers are generally used. This often leads to a bulky system with severe constraints on portability of vehicles. Hence, a breadboard circuit amplifier is developed to supply the electrical signal to the piezo ceramic actuator of the micropump. Fig. 8. shows the schematic of the proposed analog amplifier circuit. Initially this amplifier circuit is simulated using MULTISIM simulation software and then it is finally implemented in bread board.

The circuit amplifies the small amplitude sinusoidal signal of the function generator by using LT1055 amplifier arrangement. The biasing voltage is supplied by high voltage power supply circuit.

The power supply is fed from a 230V and 50Hz AC supply and it delivers a DC voltage to an amplifier circuit that is represented by the load block. The bridge rectifier transforms the sinusoidal input to a unipolar output with the pulsating waveform. Though this waveform contains a DC component, its pulsating makes it unsuitable as a DC source for amplifier circuits. Consequently, a filter is used to reduce the variation in the magnitude of the rectifier output. The output is although much more stable than that without the filter, still contains a time-dependent component, known as ripple. A voltage regulator is adopted to reduce the ripple and stabilize the magnitude of the DC output voltage against variation caused by the load current.

As seen in Fig. 9. the flow rate of the micropump increases linearly with the applied frequency, and all of the maximum flow rates occurred at the frequency of 540 Hz. The photograph of the piezo electric actuated valveless micropump is shown in Fig. 10. The analytical solution, experimental measurements and simulation results are obtained and compared. The analytical solutions of the flow rate of the micropump agree well with the INTELLISUITE software results and experimental results. For the input frequency ranging from 50 to 540 Hz, the error between the analytical solution with INTELLISUITE software result and experimental result is only 1.0 ml/min and 2.1 ml/min respectively.

6. Conclusion

In this paper, the complete design and simulation of flat walled diffuser/nozzle micropump is carried out towards the fuel delivery in a commercial 4 stroke, 125cc motorcycle using microproduct design software INTELLISUITE. The total pressure loss coefficient of the flat walled diffuser and nozzle is 1.036 and 0.28 respectively and their efficiency is 3.7. Based on this, the flow rate of the micropump is calculated theoretically as 9.89 ml/min. The maximum flow rate of the micropump is 7.2 ml/min when the driving frequency and the voltage are 540 Hz and 100 V respectively. Compared with the experimental results, the numerical simulation showed the same trend of the pumping rate as a function of actuating frequency. To further investigate this, it is fascinating to do dynamic measurements of the flow characteristics on the diffuser element. The results of this work are essential and vital for the ongoing development of piezo driven micropump for fuel delivery in small gasoline engine.

References

1. Anders Olsson, Goran Stemme, Erik Stemme: *Simulation Studies of Diffuser and Nozzle Elements for Valveless Micropumps*. In: Proceedings of the lnternational Conference on Solid-state Sensors and Actuators TRANSDUCERS ’97, 1997, Chicago, June 16-19.
2. Nisar, A., Afzulpurkar, N., Mahaisavariya, B., Tuantranont, A.: *MEMS-based micropumps in drug delivery and biomedical applications*. Sensors and Actuators B 2008, 130, 917-942.
3. Nguyen, N. T., Huang, X., Chuan, T. K.: *MEMS-Micropumps: A review*. Journal of Fluids Engineering 2002, 124, 384-392.
4. Woias, P.: *Micropumps - past, progress and future prospects.* Sensors and Actuators B 2005, 105, 28-38.
5. Van De Pol, F. C. M.: *A pump based on micro-engineering techniques.* Doctoral Thesis 1989 University of Twente Netherlands.
6. Stemme, E., Stemme, G.: *A valveless diffuser/nozzle-based fluid pump*. Sensors and Actuators A 1993, 39, 159-167.
7. Jiang, X. N., Zhou, Z. Y., Li, Y., Yang, Y., Huang, X. Y., Lin, C. Y.: *Micronozzle/diffuser flow and its application in micro valveless pumps*. Sensors and Actuators A 1998, 70, 81-87.
8. Gerlach, T.: Microdiffusers as dynamic passive valves for micropump applications. Sensors and Actuators Physics 1998, 69:181-191.
9. Chandika, S., Asokan, R.: *Design and analysis of piezoactuated micropump for fuel delivery in automobiles*. Journal of Scientific and Industrial Research 2011, 70, 448-454.
10. White, F. M.: 1986. *Fluid Mechanics*. McGraw-Hill, New York.
11. Olsson, A., Stemme, G., Stemme, E.: *A valve-less planar fluid pump with two pump chambers*. Sensors and Actuators A 1995, 46, 549-556.
12. Olsson, A., Stemme, G., Stemme, E.: *Diffuser-element design investigation for valve-less pumps*. Sensors and Actuators A 1996, 57:137-143.
13. Chandika, S., Asokan, R.: *Simulation and optimization of diffuser/nozzle micropump*. J. Sensors and Transducers 2011 (accepted for publication).
14. Singhal, V., Garimella, S. V., Murthy, J. Y.: *Low Reynolds number flow through nozzle–diffuser elements in valveless micropumps*. Sensors and Actuators A 2004, 113(2), 226-235.
15. Yang, H., Tsai, T. H., Hu, C. C.: *Portable valve-less peristaltic micropump design and fabrication*. In: Proceedings of the DTIP of MEMS & MOEMS: 9-11 April 2008, French, Riviera France.
16. Ching-Jiun Lee, Horn-Jiunn Sheen, Zhi-Kai Tu, Lei, U., Cheng-Ying Yang*: A study of PZT valveless micropump with asymmetric obstacles*. Journal of Microsystem Technology 2009, 15:993-1000.

Nomenclature

A	area of cross-section
AR	Area Ratio
C_p	Pressure recovery coefficient
d	diameter of the tube
K	Pressure loss coefficient
L	diffuser/nozzle length
W_1	throat/inlet width
W_2	exit/outlet width
2θ	Divergence angle
Δp	pressure drop
Δx	displacement
Δt	time interval
ν	mean flow velocity
Q	volume flow rate
C	flow rectifying factor
f	frequency

Subscripts

diff	diffuser
nozz	nozzle
th	throat
ex	exit
t	total
l	length

Table captions

Table 1: The loss coefficient K at different regions: (White 1986)
Table 2: Calculation of the pressure loss coefficients and diffuser efficiency for flat walled diffuser/nozzle, A_{th}=19200µm^2 and A_{ex}=72000 µm^2
Table 3: The calculated flow rate of the micropump when it is subjected to different voltages at the frequency ranges from 50 Hz to 540 Hz
Table 4 Physical Pump Parameters

Tables
Table 1

	Region 1	Region 2	Region 3
Diffuser Direction	0.05 ($K_{diff,th}$)	0.15	1.0 ($K_{diff,ex}$)
Nozzle Direction	1.0 ($K_{nozz,ex}$)	0.01	0.5 ($K_{nozz,th}$)

Table 2

	Region 1 $K_{diff,th}$	**Region 2** $K_{diff,l}$	**Region 3** $K_{diff,ex}$ **(1/AR^2)**	$K_{diff,t}$	$\eta = \frac{K_{nozz,t}}{K_{diff,\ t}}$
Diffuser	0.05	$1-\frac{1}{AR^2}-C_p$ 1- (1/3.8^2) - 0.77 =0.16	1 x (1/3.8^2) = 0.07	0.05+0.16+0.07 = **0.28**	1.036/0.28 = **3.7**
Nozzle	**Region 3** $K_{nozz,th}$ **(1/AR^2)**	**Region 2** $K_{nozz,l}$ **(1/AR^2)**	**Region 1** $K_{nozz,ex}$	$K_{nozz,t}$	
	0.5 x (1/3.8^2) 0.02	0.01 x (1/3.8^2) 0.0007	1	0.02+0.0007+1= **1.036**	

Table 3

Applied Voltage (Volt)	Frequency (Hz)	Flow rate (ml/min)
50	50	0.47
	100	0.94
	150	1.41
	200	1.87
	250	2.34
	300	2.81
	350	3.28
	400	3.75
	450	4.22
	500	4.69
	540	5.06
100	50	0.92
	100	1.83
	150	2.75
	200	3.67
	250	4.58
	300	5.49
	350	6.42

	400	7.33
	450	8.25
	500	9.17
	540	9.89

Table 4

Pump Parameters	**Proposed micropump values**
PZT material	piezo ceramic
Disc thickness t_p (mm)	0.3
Disc radius r_p (mm)	7
Thickness t_d (mm)	0.1
Radius r_d (mm)	8
Chamber radius (mm)	8
Chamber depth (mm)	0.1
Diffuser/Nozzle length (mm)	1.2
Diffuser angle (2θ)	10°
Throat/inlet width W_1	0.08
Exit/outlet width W_2	0.3
Diameter of the inlet/outlet pipe (mm)	2.4

Figure captions

Fig. 1. Schematic of the fuel injection system by piezo-ceramic actuated micropump
Fig. 2. 3D view of the piezo driven micropump
Fig. 3. Definitions of the different regions in the diffuser/nozzle element
Fig. 4. Mask layout of the proposed micropump
Fig. 5. The complete assembly of piezoelectrically actuated diffuser/nozzle micropump
Fig. 6. The calculated flow rate against the diaphragm amplitude for the flat walled diffuser
Fig. 7. Instrumentation arrangements for the flow rate test
Fig. 8. The amplifier equivalent circuit in MULTISIM
Fig. 9. The relationship between measured flow rate and applied frequency with two kinds of voltage for the valveless micropump
Fig. 10. Photograph of the piezo actuated diffuser/nozzle micropump

Figures

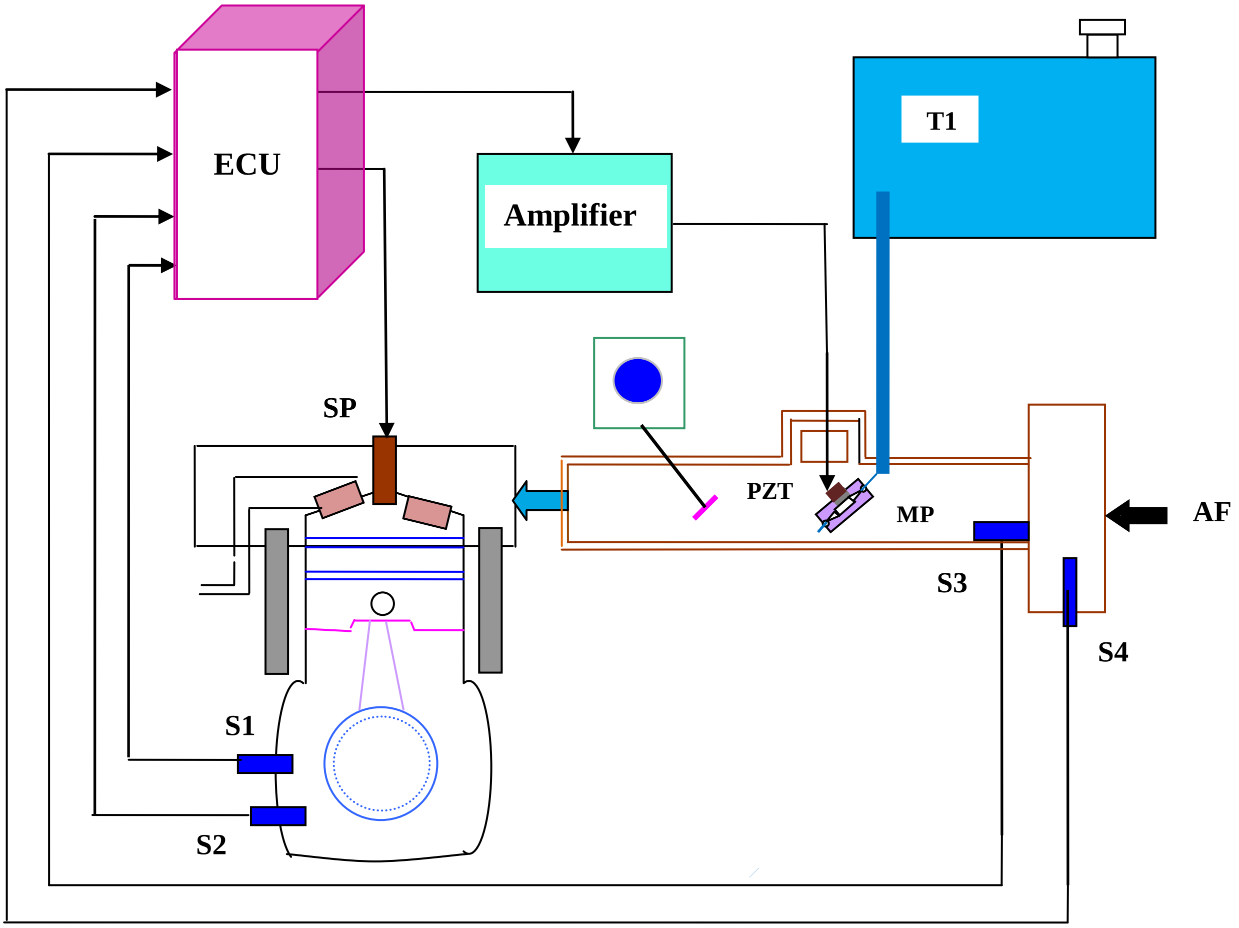

Fig. 1. T1 - fuel tank, AF - air flow, MP - micropump, PZT - piezo ceramic actuator, SP - spark plug, ECU - Electronic Control Unit, S1, S2, S3, S4 - sensors

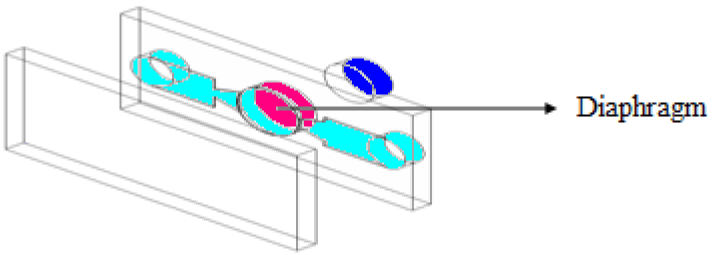

Wire frame model of micropump

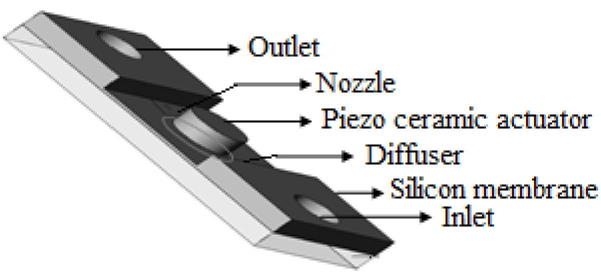

Fig. 2.

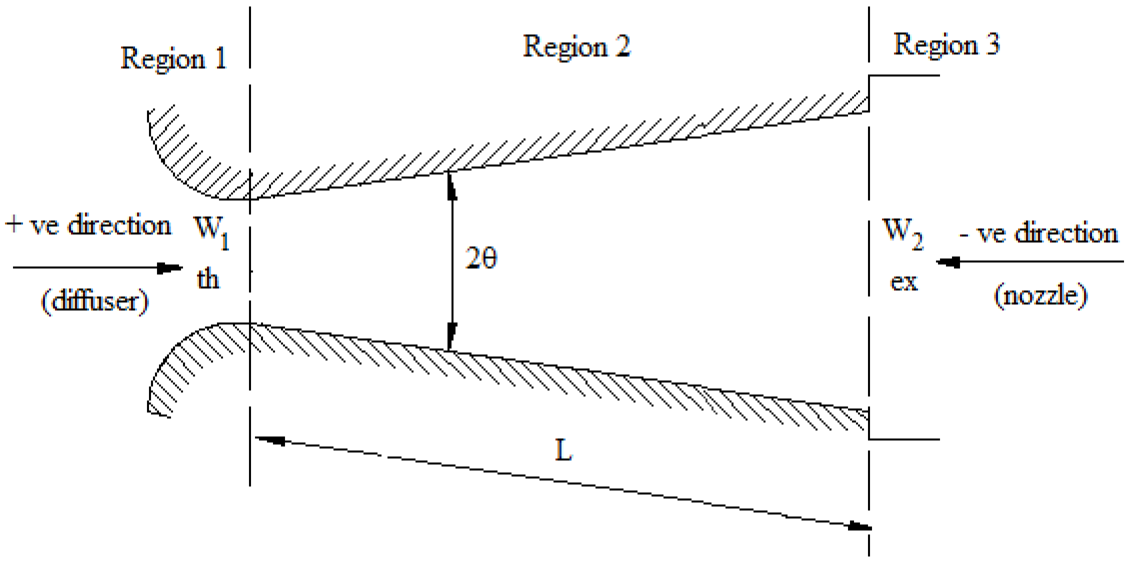

Fig. 3.

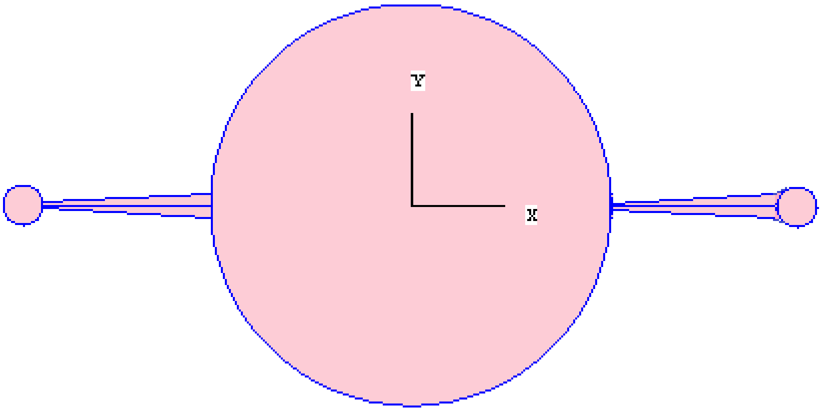

Fig. 4.

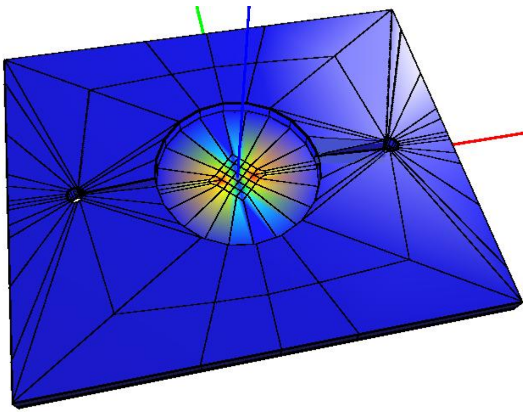
Fig. 5.

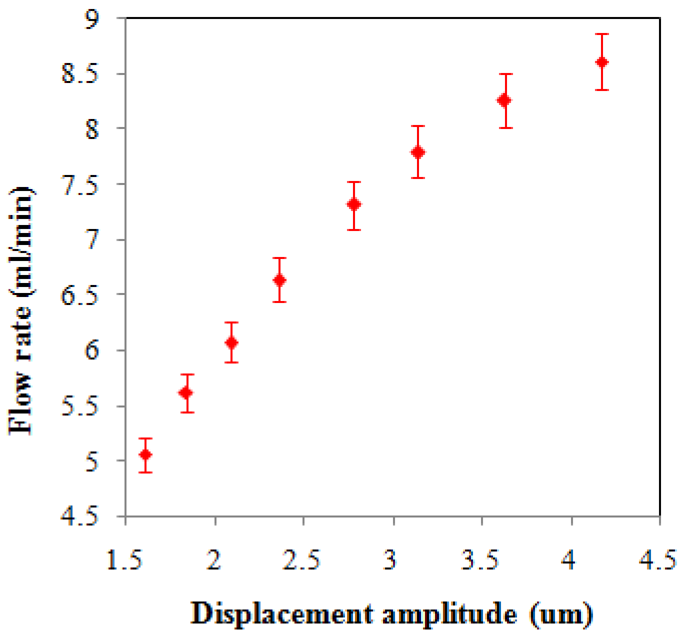

9
8.5
8
7.5
7
6.5
6
5.5
5
4.5
Flow rate (ml/min)
1.5
2
2.5
3
3.5
4
4.5
Displacement amplitude (um)

Fig. 6.

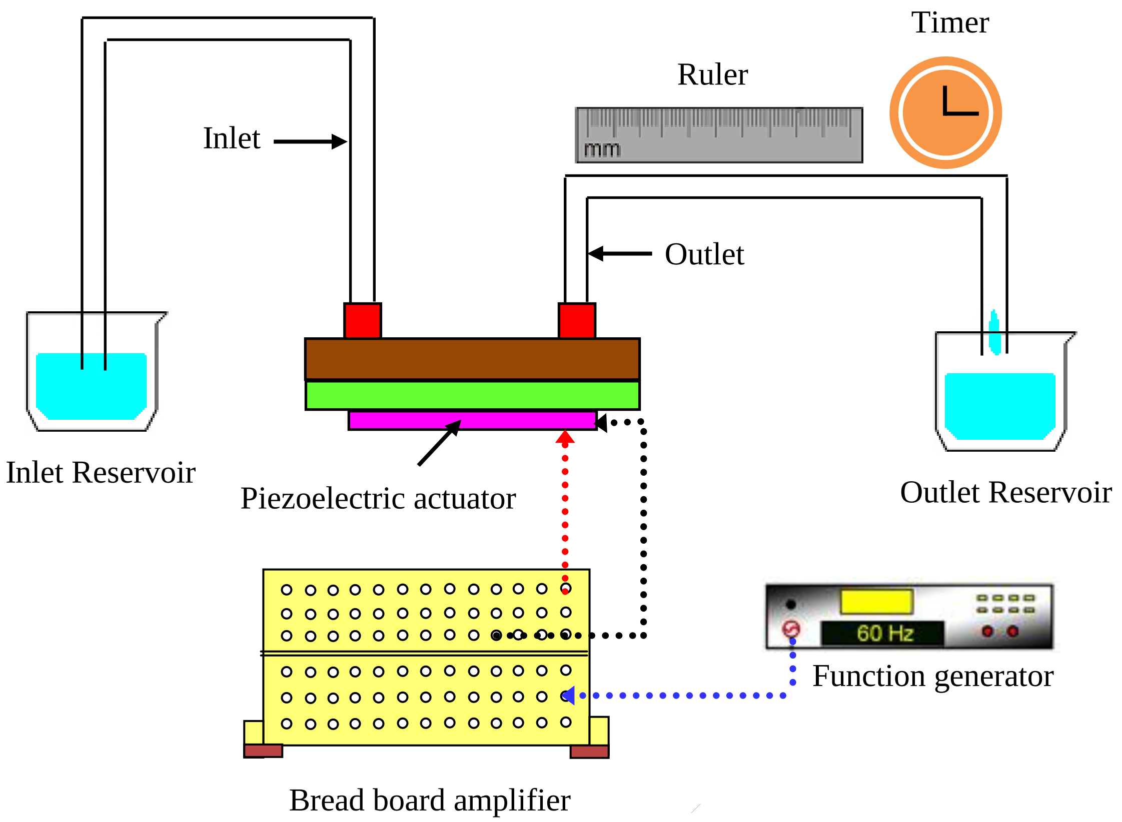

Timer
Ruler
mm
Inlet
Outlet
Inlet Reservoir
Piezoelectric actuator
Outlet Reservoir
60 Hz
Function generator
Bread board amplifier

Fig. 7.

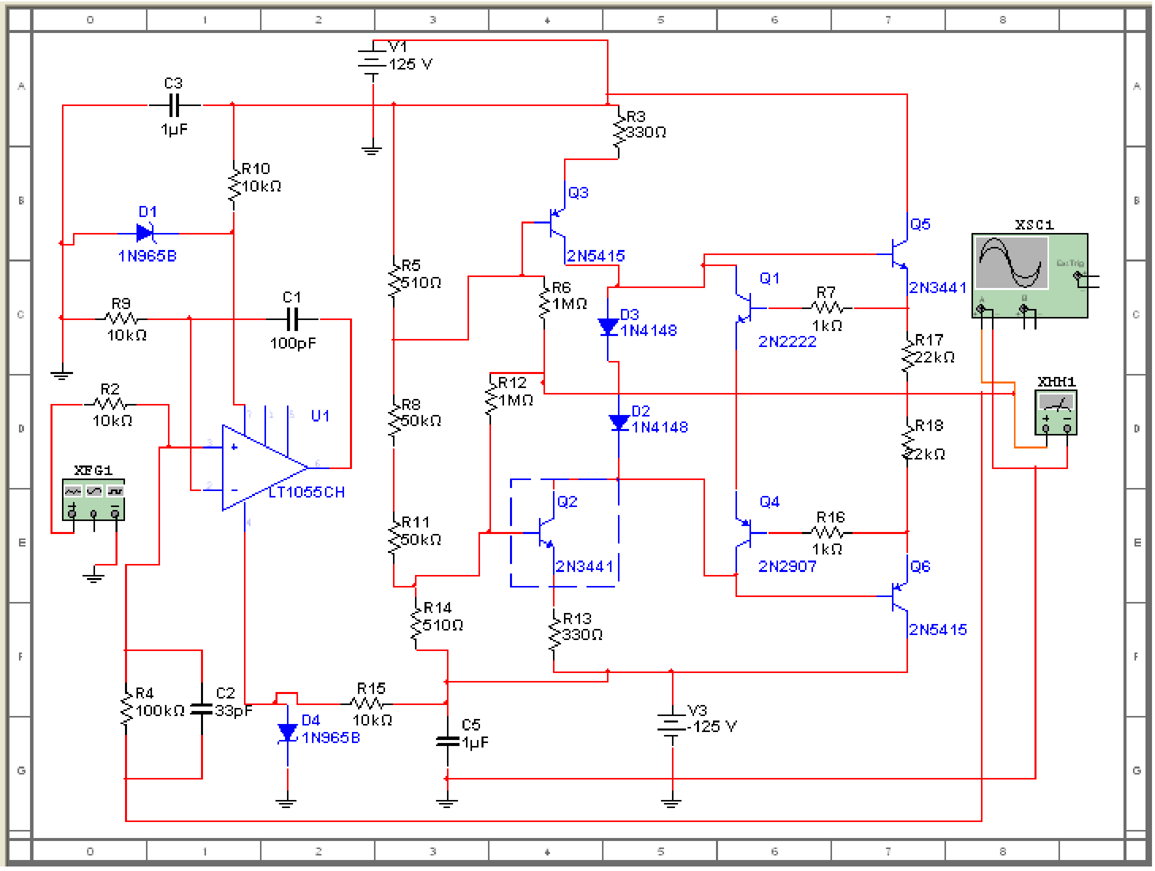
V1
125 V
C3
1µF
R3
330Ω
R10
10kΩ
Q3
D1
1N965B
2N5415
R5
510Ω
R6
1MΩ
Q1
R7
1kΩ
2N2222
Q5
2N3441
XSC1
R9
10kΩ
C1
100pF
D3
1N4148
R17
22kΩ
R2
10kΩ
R8
50kΩ
R12
1MΩ
D2
1N4148
XMM1
U1
LT1055CH
R18
22kΩ
XFG1
Q2
Q4
R16
1kΩ
R11
50kΩ
2N3441
2N2907
Q6
R14
510Ω
R13
330Ω
2N5415
R4
100kΩ
C2
33pF
D4
1N965B
R15
10kΩ
C5
1µF
V3
-125 V

Fig. 8.

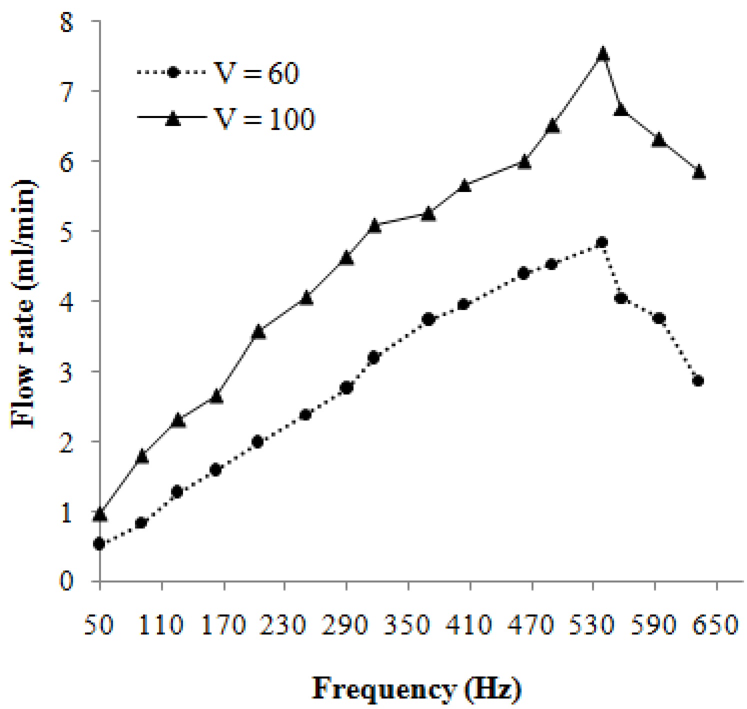
V = 60
V = 100
Flow rate (ml/min)
Frequency (Hz)
0
1
2
3
4
5
6
7
8
50
110
170
230
290
350
410
470
530
590
650

Fig. 9.

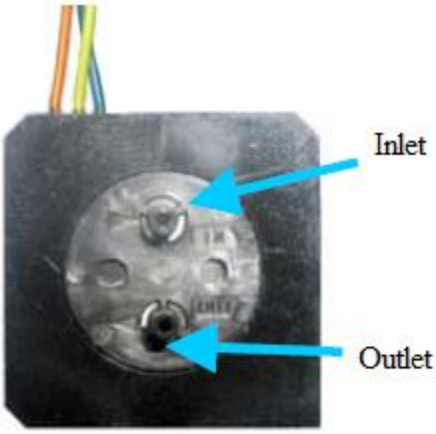

Fig. 10.